We are IntechOpen, the world's leading publisher of Open Access books Built by scientists, for scientists

5,000
Open access books available

125,000
International authors and editors

140M
Downloads

Our authors are among the

154
Countries delivered to

TOP 1%
most cited scientists

12.2%
Contributors from top 500 universities

WEB OF SCIENCE™

Selection of our books indexed in the Book Citation Index in Web of Science™ Core Collection (BKCI)

Interested in publishing with us?
Contact book.department@intechopen.com

Numbers displayed above are based on latest data collected.
For more information visit www.intechopen.com

Chapter

Theoretical Study of the Structure and Property of Ionic Liquids as Corrosion Inhibitor

Guocai Tian and Weizhong Zhou

Abstract

Three sets of ionic liquids such as 1-alkyl-3-methylimidazole chloride [$C_n$mim]Cl, 1-alkyl-3-methylimidazolium acetate [$C_n$mim]Ac and 1-octyl-3-methylimidazole salt [Omim]Y (n = 2, 4, 6, 8, and Y = Cl, BF_4, HSO_4, Ac and TFO) were used as corrosion inhibitor medium for corrosion protection of carbon steel. Electronic structures and reactivity of these ionic liquids, surface energy and electronic structures of the iron surface were systematically analyzed by density functional theory. By increasing the alkyl chain length of the [$C_n$mim]Cl and [$C_n$mim]Ac systems, the lowest unoccupied molecular orbital energy (E_{LUMO}), the highest occupied molecular orbital energy (E_{HOMO}), the softness (S) and polarizability (α) increased gradually, whereas electronegativity (χ), energy gap (ΔE), hardness (η), dipole moment (μ)and electrophilic index (ω) gradually decreased. For the [Omim]Y system, the structure parameters of ionic liquids are quite different, and only the polarizability (α) decreases gradually by increasing the length of the alkyl chain. The results show that inhibition is mainly $[C_n mim]^+$ cations of the [$C_n$mim]Cl system, and the order of inhibition efficiency follows as [C_2mim]Cl < [C_4mim]Cl < [C_6mim]Cl < [C_8mim]Cl. Both $[C_n mim]^+$ cations and the Ac^- anion have inhibition effect for the [Xmim]Ac system, and the order of inhibition efficiency is [C_8mim]Ac > [C_6mim]Ac > [C_4mim]Ac > [C_2mim]Ac. For the [Omim]Y system, $[Xmim]^+$ cations and anions (BF_4^-, HSO_4^-, Ac^-, TfO^-) have inhibition effect, and the order of inhibition efficiency is [Omim]TfO > [Omim]Ac > [Omim]HSO_4 > [Omim]BF_4 > [Omim]Cl.

Keywords: inhibitor, carbon steel, density functional theory, active site, global and local activity parameters, geometry structure

1. Introduction

Metal corrosion is a ubiquitous phenomenon in the national economy, national defense construction, science and technology and other relative fields [1–3]. It has tremendous negative effects and need to be treated. Corrosion of metal and its alloys in various fields in each country has caused serious problems in different fields and caused a series of major losses. Therefore, we must adopt effective corrosion protection measures. As latest reported from the National Association of Anticorrosive Engineers, the world's annual corrosion cost can decrease by 15–35% (US $ 375–75 billion) by adopting appropriate anticorrosion technology [1–3].

Due to its low cost and excellent physical, chemical and mechanical properties, iron and its alloys are widely used in many fields, and most of them are in contact with corrosive environments, such as tanks, pipelines, boilers, oil and gas production units and refineries [1]. Therefore, it is necessary to take certain protective measures, and the addition of an inhibitor can significantly reduce the corrosion rate of iron and ferroalloy, and the amount of inhibitor is small, which has become an economic and effective method [2]. Traditional inhibitors, such as chromate, nitrite, silicate and molybdate, can react with metals to constitute a passive film or a dense metal salt protective film on the metal surface, preventing the corrosion of metals and alloys [3]. However, this kind of inhibitor is usually used in large amount and high cost. In addition, when the amount of inhibitor is insufficient, it will lead to serious local corrosion of metals and alloys. In addition, these inhibitors have certain toxicity and poor biodegradation ability. When they are accustomed, there are serious environmental and ecological problems and they are increasingly restricted. Therefore, it is very important to develop environment-friendly inhibitors. As an environment-friendly inhibitor, imidazolines, amides and other inhibitors have the characteristics of high efficiency, low toxicity and easy biodegradation, which are commonly used in the corrosion inhibition of iron and alloy [1–3].

In recent years, ionic liquids (ILs) as a new green solvent, which is formed by organic cations with various inorganic or organic anions, have attracted more and more attention [4–6]. Due to the heterocyclic structure, heteroatoms (such as N, O and S) and multiple bonds in ionic liquid molecules, they have become effective inhibitors and are commonly used in the field of corrosion protection [6–9]. The ionic liquid common inhibitors are imidazole ionic liquid, pyridine ionic liquid and quaternary ammonium ionic liquid. Compared with traditional corrosion inhibitors, ionic liquid corrosion inhibitors are always renewable, inexpensive, ecologically acceptable, readily available and environmentally friendly and biodegradable. Various ionic liquids such as imidazoline, pyridine, ammonium, pyridazine and benzimidazole were widely used as corrosion inhibitors for carbon steel. The experimental methods such as surface analysis techniques, electrochemical tests and electrochemical impedance spectroscopy are used extensively to study the performance of ionic liquid inhibitors [9–25].

However, experimental research on ionic liquid inhibitors mainly focuses on the evaluation of their corrosion inhibition performance. The research on the corrosion inhibition mechanism of ionic liquid inhibitors is less, which can not reveal some details of the corrosion inhibition process, such as the quantitative description of the molecular metal atom combination of inhibitors, the determination of the functional groups of inhibitors and the information on the process of ion adsorption and film formation of inhibitors [9–11]. It is impossible to guide the development of ionic liquid inhibitors by obtaining and diffusing the inhibitors on the metal surface. Therefore, it is necessary to study the mechanism of ionic liquid inhibitors by theoretical calculation, so as to provide theoretical guidance for the development and application of new and efficient ionic liquid inhibitors.

With the rapid improvement and advancement of computer science and technology, and the gradual improvement of related theories, quantum chemical calculation as an important theoretical calculation method has been proved to be very effective in determining the electronic structure of molecules and clarifying the reaction activity of molecules. The inhibition mechanism and performance of inhibitors are often the same as the electronic structure and reaction activity of inhibitors. Therefore, it is very important to study the electronic structure and reaction activity of ionic liquid inhibitors for the design of new ionic liquid inhibitors [26]. Murulana et al. [27] studied 1-octyl-3-methylimidazolium bis

(trifluoromethyl-sulfonyl) imide ([Hmim]NTF_2), 1-propyl-3-methylimidazolium-bis(trifluoromethyl-sulfonyl) imide ([Pmim]NTF_2), 1-propyl-2,3-dimethylimidazolium bis(trifluoromethyl-sulfonyl) imide [PDmim]NTF_2 and 1-butyl-3-methylimidazolium bis(trifluoromethyl-sulfonyl) imide ([Bmim]NTF_2). The results showed that [PDmim]NTF_2 has the strongest capability of electron donor, and [Pmim]NTF_2 has capability of electron acceptor. The active centers are located in the ring of imidazole cation and the N and O atoms of anions. Sasikumar et al. [28] studied the behavior of 1-decyl-3-methylimidazolium tetrafluoride ([Dmim]BF_4), 1-ethyl-3-methylimidazolium boron tetrafluoride ([Emim]BF_4) and 1-butyl-2,3-dimethylimidazolium tetrafluoride ([BDmim]BF_4) inhibition on low carbon steel by density functional theory in hydrochloric acid solution. The results showed that the variations of the E_{HOMO}, hardness (η) and dipole moment (μ) are in agreement with the electrochemical experiments. The order of inhibition efficiency is [Dmim]BF_4 > [BDmim]BF_4 > [Emim]BF_4, which agrees well with experiments. The corrosion inhibition behavior of 1-hexyl-3-methylimidazolium iodide ([Hmim]I), 1-hexyl-3-methylimidazolium phosphorus hexafluoride ([Hmim]PF_6), 1-hexyl-3-methylimidazolium trifluoromethanesulfonate ([Hmim]TFO) and 1-hexyl-3-methylimidazolium boron tetrafluoride ([Hmim]BF_4) on carbon steel was studied by Mashuga et al. [29] with density functional theory. It was found that the variation order of E_{HOMO}, hardness (η), softness (S) and the dipole moment (μ) is [Hmim]PF_6 < [Hmim]BF_4 < [Hmim]I < [Hmim]TFO. The results agree well with the experimental inhibition efficiency measured by electrochemical methods. The inhibition performance of two 1-ethyl-3-methylimidazolium-based ionic liquids formed with ethyl sulfate ([Emim]$EtSO_4$) and acetate ([Emim]Ac) and three 1-butyl-3-methylimidazolium-based ionic liquids with acetate ([Bmim]Ac), thiocyanate ([Bmim]SCN) and dichloride ([Bmim]DCA) on carbon steel in acid medium was studied with density functional theory by Yesudass et al. [30]. The results show that the inhibition efficiency follows [Emim]Ac < [Bmim]SCN < [Bmim]Ac < [Bmim]DCA < [Emim]$EtSO_4$, which is consistent with the experimental results.

As mentioned above, although some progress has been made in the study of the corrosion mechanism and properties of low carbon steel by ionic liquid corrosion inhibitors in the corrosion medium, there are still some problems. Experimental methods (weight-loss method, electrochemical experiment method and surface morphology analysis method) are used to study the ionic liquid, mainly focusing on the evaluation of the inhibition performance and efficiency of ionic liquid, but it is difficult to know the inhibition mechanism of ionic liquid on the iron surface. However, the structure parameters calculated by quantum chemistry are not systematically analyzed. For example, for the imidazole system with different cations, how do the structure parameters and property change with the increase of the cationic alkyl chain length? For the system with the same cations and different anions, how do the structure parameters change? There is no systematic analysis of the properties of different surfaces of iron, but it simply selects a surface as the adsorption surface of ionic liquid. At the same time, different surface of iron may have different electric charge and different electric charge. There are some relations between iron and HOMO and LUMO of ionic liquid molecules, but there are few related researches.

Molecular simulation is only a simple calculation of adsorption energy between the metal surface and ionic liquid inhibitors, but there are few studies on the quantitative description of the molecular metal atom combination of ionic liquid, the determination of the functional groups of ionic liquid, and the acquisition of the process information of adsorption and film formation, which cannot guide the development of ionic liquid corrosion inhibitors. In this paper, the equilibrium geometry, frontier orbit, global and local reactivity of [$C_n$mim]Cl system, [$C_n$mim]Ac system and

[Omim]Y (n = 2, 4, 6, 8, Y = Cl, BF_4, HSO_4, Ac and TFO) are studied by quantum chemical calculation. The active region, inhibition efficiency of possible interaction between ionic liquid molecules and iron surface are preliminaries analyzed.

2. Computational method

The B3LYP method of density functional theory in Gaussian 09 software package [31] is utilized to optimize the geometric configuration and analyze the frequency of ionic liquid. The 6-311++G(d, p) basis set was used in this paper, which is same as the literature [26–28]. The geometry optimization and frequency analysis of the studied ionic liquid molecules were performed, and the stable geometry was obtained. There are seven interaction sites of 1-alkyl-3-methylimidazolium cations to interact with anions, as shown in **Figure 1**, where 1–5 represent the five positions of anions in the plane of imidazole ring, and 6 and 7 are respectively located on both sides perpendicular to the plane of imidazole ring. As confirmed by many authors, position 2 is the most active site and the anions are always located in this position, so we just discuss the anions' contact with cations at position 2. The E_{HOMO} and E_{LUMO}, energy gap (ΔE), electronegativity (χ), the softness (S), dipole moment (μ), polarizability (α), electrophilic index (ω), hardness (η), Fukui index and other structural and property parameters were calculated. Distribution of Fukui index was drawn by Multiwfn software [32, 33].

According to the frontier molecular orbital theory, the molecules' reactivity is related to their lowest unoccupied molecular orbits (LUMO) and the highest occupied molecular orbital (HOMO). In general, the level of the E_{HOMO} value determines the ability to deliver electrons to the outside. The level of the E_{LUMO} value represents the ability to obtain electrons. Therefore, the higher the E_{HOMO} value, the lower the E_{LUMO} value can reflect the reactivity of a molecule. [34] As for the adsorption of a molecule on the carbon steel surface, a higher E_{HOMO} value will make them have a stronger electronic supply capacity and can form an adsorption with the d orbital on the surface of iron. A lower E_{LUMO} value will make them have a stronger electronic acceptance capacity, which becomes more easily accepted electrons from the surface of iron and form an antibond orbital to promote the adsorption. Therefore, the energy gap difference $\Delta E = E_{HOMO}$-E_{LUMO} can be used to assess

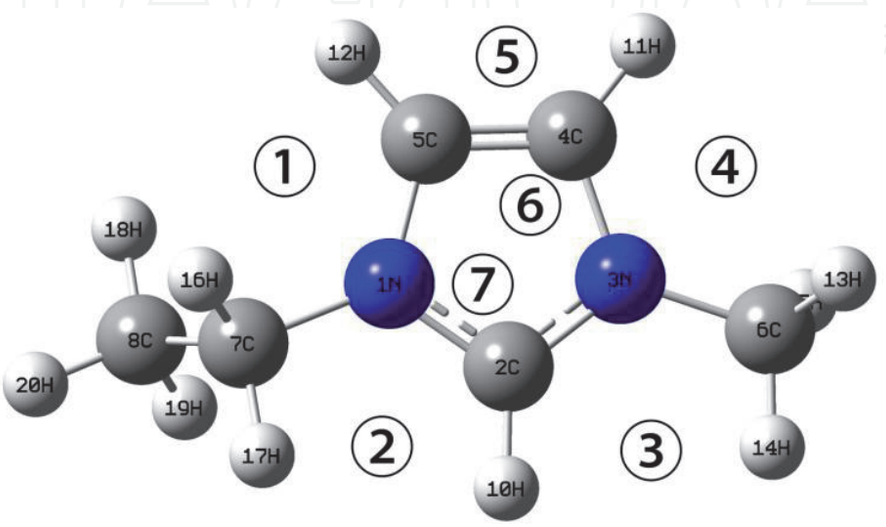

Figure 1.
Anions can form ionic liquids with $[Emim]^+$ in several different sites.

the bonding ability of a molecule with iron. The smaller Δ_E is, the stronger bonding ability with iron is, and the easier adsorption on the iron surface [35].

In the concept density functional theory, according to Koopmans theorem [36], ionization potential I under vacuum condition can be approximated to the negative value of E_{HOMO} $I = -E_{HOMO}$. Similarly, the electron affinity a is approximately negative for E_{LUMO} $A = -E_{LUMO}$. The dipole moment (μ), electronegativity (μ), softness (S) and polarizability (α) of a molecule are generally referred to as the global reactivity of a molecule [37, 38]. Molecular polarity is always described by dipole moment (μ), which is defined as the product of atomic distance R and atomic charge q as $\mu = qR$ [39]. Generally, the higher μ will make the molecules more easily adsorbed on the surface of carbon steel [40], and the efficiency of the molecular inhibitor will increase accordingly. However, the dipole moment reflects the global polarity of molecules rather than the polarity of the bond in the molecule. According to the concept density functional theory, the electronegativity (χ) of the system with n electrons is defined as follows when the external field $\nu(r)$ is fixed [38]:

$$\chi = -\left(\frac{\partial E}{\partial N}\right)_{\nu(r)} \tag{1}$$

Hardness (η) is defined as the second derivative of the system energy E to N [41]

$$\eta = \frac{1}{2}\left(\frac{\partial^2 E}{\partial N^2}\right)_{\nu(r)}. \tag{2}$$

Using the finite difference approximation, the global hardness (η) and electronegativity (χ) are related to ionization energy I and affinity energy A as follows [42]:

$$\chi = \frac{I + A}{2}, \tag{3}$$

$$\eta = \frac{I - A}{2} \tag{4}$$

According to Koopmans theorem [36], the electronegativity (χ) and global hardness (η) can be calculated from E_{HOMO} and E_{LUMO} as

$$\chi = -\frac{E_{HOMO} + E_{LUMO}}{2}, \tag{5}$$

$$\eta = \frac{E_{LUMO} - E_{HOMO}}{2}. \tag{6}$$

Global softness (s) is usually defined as the reciprocal of global hardness [37].

$$S = \frac{1}{\eta}. \tag{7}$$

Electronegativity (χ) is a scale of the ability of atoms in molecules to attract electrons. The larger its value is, the easier it is to attract electrons [38] reflecting a better inhibitor effect. The smaller the global hardness (η) or the larger the global softness (S) of the molecule means that the stronger the interaction between metal surface and a molecule [43], and a higher corrosion inhibition efficiency. Parr introduced the concept of electrophilic index (ω), which is defined as following [37]:

$$\omega = \frac{\chi^2}{2\eta}. \tag{8}$$

According to the definition, this parameter is a measure of the capability of electron acceptors. The larger the value is, the stronger the capability of electron acceptor is. As an important parameter of global reaction activity, the molecular polarizability (α) is the average value obtained by calculation, and its relationship is as follows [44]:

$$\alpha = \frac{1}{3}\left(\alpha_{xx} + \alpha_{yy} + \alpha_{zz}\right). \tag{9}$$

where, α_{xx}, α_{yy} and α_{zz} are molecular polarizability in x, y and z directions, respectively. The higher the molecular polarizability (α) is, the easier adsorption on the metal surface is, and the higher corrosion inhibition performance is [44].

The local reactivity of ionic liquid inhibitors was evaluated by their Fukui index. Nucleophilic and electrophilic behavior of the molecule was studied by analyzing its Fukui index distribution. Fukui function is an important concept in density functional theory, which is commonly used to predict the active sites of a molecule [45]. In the case of certain outfield $v(r)$, the Fukui function is defined as follows [46]:

$$f(r) = \left[\frac{\partial \rho(r)}{\partial N}\right]_{v(r)}. \tag{10}$$

Within the finite difference approximation, the nucleophilic attack can be expressed as $f^+(r) = \rho_{N+1}(r) - \rho_N(r)$, and electrophilic attack is $f^-(r) = \rho_N(r) - \rho_{N-1}(r)$ [29], where $\rho_{N+1}(r)$、 $\rho_N(r)$、 $\rho_{N-1}(r)$ are the charge density of the atom in the molecule with one unit negative charge, uncharged and one unit positive charge, respectively.

3. Results and discussion

3.1 1-Alkyl-3-methylimidazole chloride [$C_n$mim]Cl

In this section, we will analyze the equilibrium geometry, frontier orbital distribution, global and local reactivity, the change rule of the reactive sites and structure parameters of ionic liquids with the increase of the cationic alkyl chain length for the [$C_n$mim]Cl system. The comparison of the corrosion inhibition performance was achieved for the ionic liquids formed with the same anion and different cations.

3.1.1 Equilibrium geometry structures, HOMO and LUMO

Figure 2 shows the equilibrium geometry, HOMO and LUMO distribution of [$C_n$mim]Cl (n = 2, 4, 6, 8) system obtained by B3LYP/6-311++G(d, p) method. It can be seen from **Figure 2** that the equilibrium geometry HOMO and LUMO profiles of these four ionic liquids are very similar. The anions are all at the C2 atom of the imidazole ring. HOMO is distributed on anions, but not on cations, which indicates that Cl^- is easy to form a coordination bond with d-orbital on an iron surface, while imidazole ring is not easy to provide electrons and interact with the iron surface. LUMO is mainly distributed on the imidazole ring, and other C atoms and anions of cation also have little distribution, which indicates that the imidazole

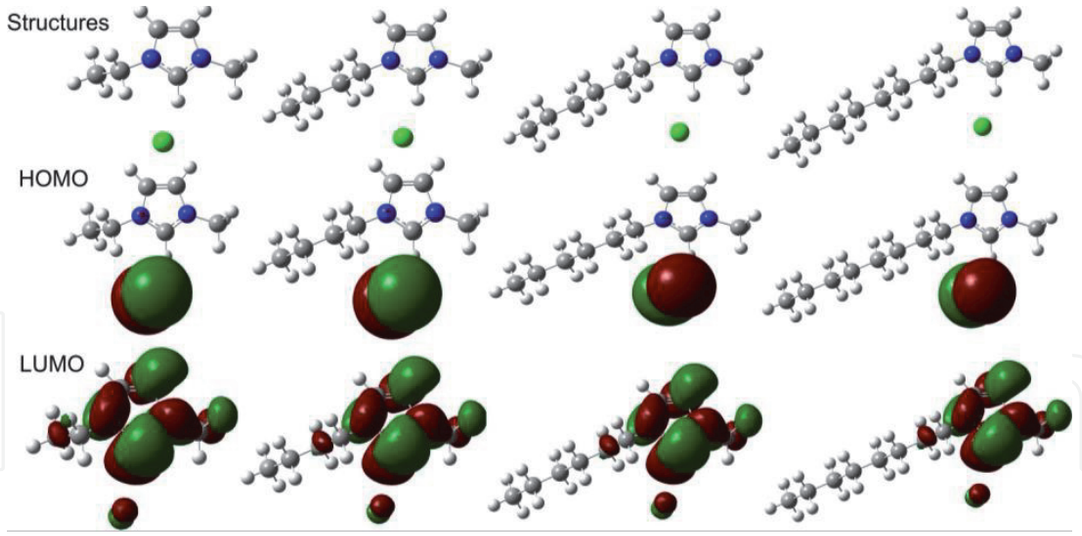

Figure 2.
The equilibrium geometry structures, HOMO and LUMO isosurfaces of [$C_n$mim]Cl (n = 2,4,6,8) with B3LYP/6-311++G(d,p) method. From left to right, it is [C_2mim]Cl, [C_4mim]Cl, [C_6mim]Cl and [C_8mim]Cl, respectively.

ILs	[C_2mim]Cl	[C_4mim]Cl	[C_6mim]Cl	[C_8mim]Cl
E_{HOMO} (eV)	−5.2672	−5.2641	−5.2623	−5.2608
E_{LUMO} (eV)	−1.1890	−1.1824	−1.1820	−1.1819
ΔE (eV)	4.0782	4.0817	4.0903	4.0789

Table 1.
E_{HOMO}, E_{LUMO} *and* ΔE *of* [$C_n$mim]Cl *(n = 2, 4, 6, 8) with B3LYP/6-311++G (d, p) method.*

ring of cation is easy to accept electrons from the iron surface and form a feedback bond. According to the distribution of HOMO and LUMO, when the [Xmim]Cl ionic liquid adsorbs on the surface of carbon steel, the imidazole ring of the ionic liquid will interact with the surface of carbon steel and lay parallel to the surface.

The E_{HOMO}, the E_{LUMO} and the energy gap difference (ΔE) of four ionic liquid molecules in [$C_n$mim]Cl system are shown in **Table 1**. It can be seen from **Table 1** that by increasing the length of the alkyl chain, the E_{HOMO} becomes larger and larger, indicating the increased capability of electron donor of the molecule. By increasing the length of the alkyl chain, E_{LUMO} also has an increasing trend, which shows that the capability of electron acceptor will weaken. However, the smaller (ΔE) is, the better the activity of the molecule is, the easier absorption between the carbon steel surface and molecules, and the higher the inhibition efficiency is. The sequence of inhibition efficiency of these four ionic liquids should be [C_2mim]Cl < [C_4mim]Cl < [C_6mim]Cl < [C_8mim]Cl. The [C_8mim]Cl has the highest inhibition efficiency and the best inhibition performance, which agrees well with the experimental measurement [29].

3.1.2 Global activity parameters

Table 2 shows the global activity parameters of [$C_n$mim]Cl system obtained by B3LYP/6-311++G(d, p) method. It can be seen from **Table 2** that by increasing the length of the alkyl chain, the dipole moment (μ) decreases gradually, indicating that the increase in alkyl chain length will reduce the polarity of the whole molecule. Increasing the length of alkyl chain, the electronegativity (χ) is also gradually

ILs	μ/Debye	χ/eV	η/eV	S/eV^{-1}	ω/eV	α(a.u.)
[C_2mim]Cl	12.6974	3.2281	2.0391	0.4904	2.5552	117.8930
[C_4mim]Cl	12.3672	3.2232	2.0409	0.4900	2.5453	132.8403
[C_6mim]Cl	12.2509	3.2222	2.0402	0.4902	2.5445	158.3847
[C_8mim]Cl	12.2083	3.2213	2.0394	0.4903	2.5441	183.8247

Table 2.
Global activity parameters for [$C_n$mim]Cl (n = 2, 4, 6, 8) system with B3LYP/6-311++G(d,p) method.

reduced, which indicates that the ability of molecules to attract electrons is weaker and weaker, which is not conducive to accepting the electrons on the iron surface. The global hardness (η) of the molecules decreases, while the global softness (S) increases by increasing the chain length, which indicates that the interaction between the surface of carbon steel with the molecules becomes stronger and stronger, and the molecules tend to adsorb on the surface. The electrophilic index (ω) decreases by increasing the length of the alkyl chain. With the lowest unoccupied molecular orbital energy (E_{LUMO}), the ability of the molecule to accept electrons becomes weaker and weaker. Molecular polarizability (α) is an important quantum chemical parameter in the field of corrosion protection. From **Table 2**, the order of the magnitude of [C_8mim]Cl > [C_6mim]Cl > [C_4mim]Cl > [C_2mim]Cl can be concluded, indicating that [C_8mim]Cl is most easily adsorbed on the surface of iron and its corrosion inhibition efficiency is the highest. According to the analysis results in Section 3.1.1, with the increase of the alkyl chain length, the global activity parameters of [$C_n$mim]Cl system, such as global hardness (η), global softness (S) and polarizability (α), increases; therefore, the corrosion inhibition efficiency increases [29].

3.1.3 Local activity parameters

Figure 3 shows the Fukui index f^- distribution of four ionic liquid molecules in [$C_n$mim]Cl system, with the electrophilic attack index distribution on the left and the nucleophilic attack index f^+ distribution on the right. It can be seen from **Figure 3** that the electrophilic attack index of these four ionic liquid molecules is mainly distributed on the Cl atom with the HOMO.

It is easy to provide electrons when attacked by the dielectric since Cl atom has high electronegativity and high electron density around them. As the same of distribution of LUMO, the nucleophilic attack index of these four kinds of ionic liquid molecules is mainly distributed on the imidazole ring, especially 2C, 4C, 5C and 1N atoms (see **Figure 1** for the number of specific atom). The imidazole ring is

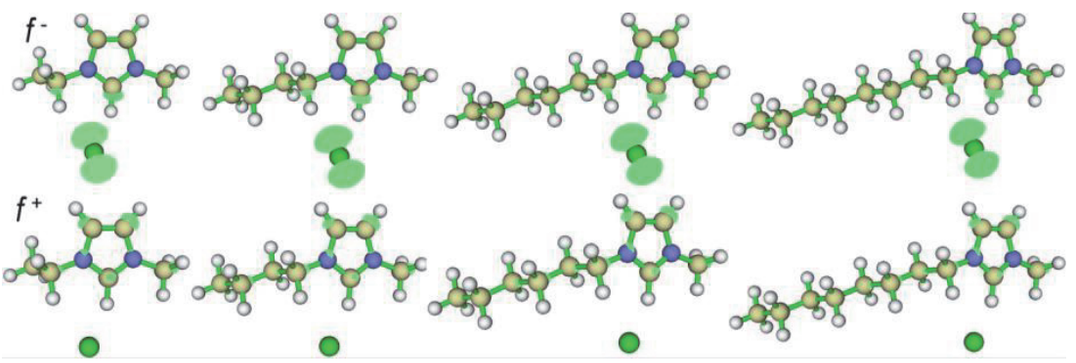

Figure 3.
Fukui indices isosurfaces of [$C_n$mim]Cl (n = 2, 4, 6, 8) system with B3LYP/6-311++G(d,p) method. The [C_2mim]Cl, [C_4mim]Cl, [C_6mim]Cl and [C_8mim]Cl are shown from left to right, respectively.

positively charged, and it is easier to accept electrons when attacked by the nucleophilic medium. Therefore, local reactive sites of [$C_n$mim]Cl are Cl, 2C, 4C, 5C and 1N atoms (see **Figure 1** for the number of specific atom), which are easy to interact with iron surface and adsorb on iron surface.

3.2 1-Alkyl-3-methylimidazolium acetate [$C_n$mim]Ac system

In this part, we will discuss how the change of chain length affects the change of structure and property of [$C_n$mim]Ac (n = 2, 4, 6, 8) system with the same anion and different cations through the density functional theory. The equilibrium geometry, frontier orbital distribution, global reactivity and local reactivity, the change rule of reactive sites and structure parameters of ionic liquids by increasing the length of cationic alkyl chain and the comparison of corrosion inhibition performance are obtained and analyzed. In addition, the influence of different anions Cl^-, Ac^- on the reaction activity of ionic liquids was analyzed by comparing [$C_n$mim]Ac (n = 2, 4, 6, 8) system with [$C_n$mim]Cl system.

3.2.1 Equilibrium geometry and frontier orbital distribution

Figure 4 shows the equilibrium geometry, HOMO and LUMO frontier molecular orbital distribution of [$C_n$mim]Ac (n = 2, 4, 6, 8) system obtained by B3LYP/6-311++G(d,p) method. It can be seen from **Figure 4** that the equilibrium geometry HOMO and LUMO distribution for these four ionic liquids is very similar. The anion Ac^- is located under the cation, and the optimized C—O bond is a double bond. HOMO is mainly distributed on the anion Ac^-, especially O atom, while C atom on the cation also has a small contribution, which shows that the unpaired O atom on the anion easily forms a coordination bond with the empty d-orbital on the iron surface and adsorbs on the iron surface. LUMO is mainly distributed on the imidazole ring, and there is a small amount of C of other cations and anions, which shows that the imidazole ring of cations easily accepts electrons from the iron

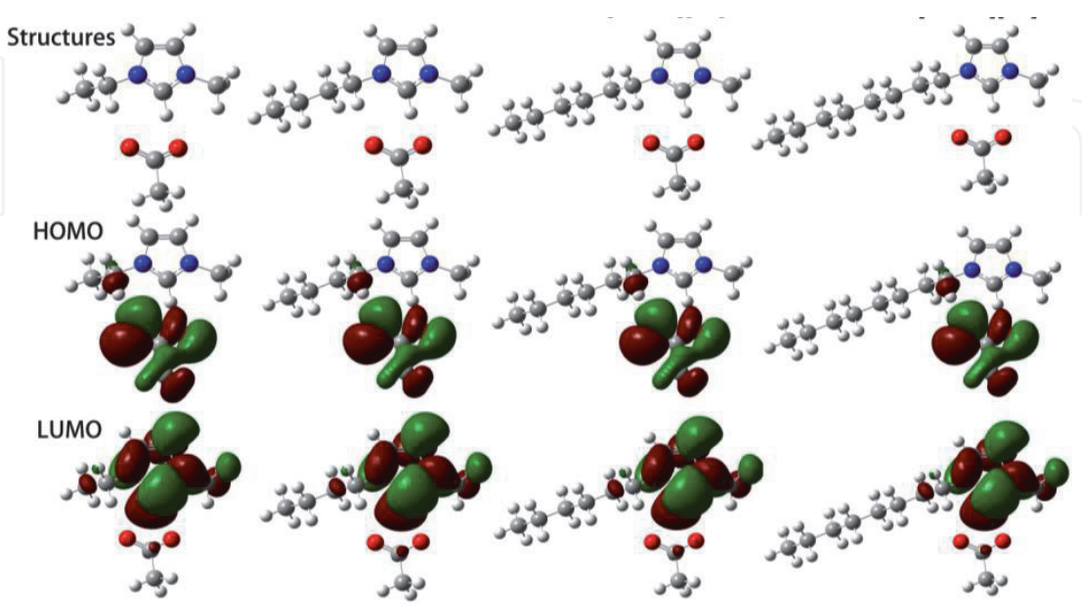

Figure 4.
Equilibrium geometry structures, HOMO and LUMO isosurfaces of [$C_n$mim]Ac (n = 2, 4, 6, 8) system with B3LYP/6-311++G(d, p) method. From left to right, it is [C_2mim]Ac, [C_4mim]Ac, [C_6mim]Ac and [C_8mim]Ac, respectively.

surface, forming a feedback bond, which makes the imidazole ring easy to be adsorbed on the iron surface.

The E_{HOMO}, E_{LUMO} and the energy gap ΔE of four [$C_n$mim]Ac (n = 2, 4, 6, 8) ionic liquid are shown in **Table 3**. It is shown in **Table 3** that E_{HOMO} and E_{LUMO} increase as that of [$C_n$mim]Cl (n = 2, 4, 6, 8) in **Table 2**, by increasing the length of alkyl chain, indicating that the capability of electron donator enhances and the capability of electron acceptor weakens. However, the smaller ΔE is, the better the activity of the molecule is, the easier it is to be adsorbed on the surface of iron and the better the inhibition effect is. The sequence of inhibition efficiency of the four ionic liquids should be [C_8mim]Ac > [C_6mim]Ac > [C_4mim]Ac > [C_2mim]Ac, and the inhibition efficiency of [C_8mim]Ac is the highest. The order obtained is the same as that of system analysis.

3.2.2 Global active parameters

Table 4 shows the global active parameters of [$C_n$mim]Ac system obtained by B3LYP/6-311++G(d,p) method. It can be seen from **Table 4** that by increasing the length of the alkyl chain, the dipole moment (μ) decreases gradually. Increasing the alkyl chain length will reduce the polarity of the whole molecule. The electronegativity (χ) also decreases gradually, which indicates that the capability of attracting electrons is weaker and weaker, and is not conducive to receiving electrons on the iron surface. This results are the same as those of [$C_n$mim]Cl system. As the alkyl chain length increases, the global hardness (η) and the global softness (S) of the molecule decrease, which indicates a stronger interaction between the carbon surface with the molecule and the molecule is more stably adsorbed on the iron surface. The electrophilic index (ω) decreases by increasing the alkyl chain length. With the increase of E_{LUMO}, the capability of electron acceptor of a molecule is weaker and weaker.

It can be seen from **Table 4** that the order of α is [C_8mim]Ac > [C_6mim]Ac > [C_4mim]Ac > [C_2mim]Ac, indicating that [C_8mim]Ac is most easily adsorbed on the iron surface. So, [C_8mim]Ac should have the best inhibition effect and the highest inhibition efficiency. Similar to the [$C_n$mim]Cl system, by increasing the length of alkyl chain, the values of dipole moment (μ), electronegativity (χ), global

ILs	[C_2mim]Ac	[C_4mim]Ac	[C_6mim]Ac	[C_8mim]Ac
E_{HOMO}	−5.4007	−5.3992	−5.3951	−5.3943
E_{LUMO}	−0.9120	−0.9009	−0.8979	−0.8985
ΔE	4.4887	4.4982	4.4972	4.4958

Table 3.
E_{HOMO}, E_{LUMO} *and* ΔE*(eV)of [*C_n*mim]Ac (n = 2, 4, 6, 8) with B3LYP/6-311++G(d, p) method.*

ILs	μ/Debye	χ/eV	η/eV	S/eV^{-1}	ω	α(a.u.)
[C_2mim]Ac	9.9354	3.1563	2.2444	0.4456	2.2194	120.9223
[C_4mim]Ac	9.6985	3.1500	2.2491	0.4446	2.2059	146.3850
[C_6mim]Ac	9.6243	3.1465	2.2486	0.4447	2.2015	171.8383
[C_8mim]Ac	9.5918	3.1464	2.2479	0.4449	2.2020	197.2063

Table 4.
Global activity parameters for [C_n*mim]Ac (n = 2, 4, 6, 8) system with B3LYP/6-311++G(d,p) method.*

hardness (η) and electrophilic index (ω) decrease, while the global activity parameters global hardness (η), global softness (S) and polarizability (α) increase. The order of polarization (α) is in agreement with that of corrosion inhibition efficiency.

3.2.3 Fukui index distribution

Figure 5 shows the Fukui index distribution of four ionic liquid [$C_n$mim]Ac systems. It can be seen from **Figure 5** that the electrophilic attack index of these four ionic liquid molecules is mainly distributed on the anion Ac^-, especially O atom, and the cation also has a small amount of distribution, indicating that the anion containing oxygen group is easy to provide the d-orbital combination of electron and iron surface space, and can stably be adsorbed on the iron surface. The nucleophilic attack index is mainly distributed in 2C, 4C and 5C atoms in imidazole ring (the number of atoms is shown in **Figure 1**) and O atom of anion, indicating that both cations and anions of [$C_n$mim]Ac system will interact with the surface of iron, making the adsorption of molecules on the surface of iron more stable. So the local reactive sites of [$C_n$mim]Ac are placed in O, 2C, 4C, 5C and 1N atoms. Local reactive sites are almost the same for [$C_n$mim]Ac and [$C_n$mim]Cl, except for Cl in [$C_n$mim]Cl.

3.3 1-Octyl-3-methylimidazole [Omim]Y system

In this section, we will discuss the structure and property of [Omim]Y (Y = Cl, BF_4, HSO_4, Ac, TFO) ionic liquids formed with the same cation and different anions. The equilibrium geometry, frontier orbital distribution, global reactivity and local reactivity, the change of reactive sites, structure parameters and corrosion inhibition performance of ionic liquids with different anions are obtained and discussed.

3.3.1 Equilibrium geometry and frontier orbital distribution

Figure 6 shows the equilibrium geometry, HOMO and LUMO distribution of [Omim]Y system obtained by B3LYP/6-311++G(d, p) method. It can be seen from **Figure 6** that the equilibrium geometry of the four ionic liquids is very similar, and the anions are all under the cations. LUMO is mainly distributed on the imidazole ring in the same way as [$C_n$mim]Cl system and [$C_n$mim]Ac system, which indicates that the imidazole ring of cation can easily accept electrons from the iron surface

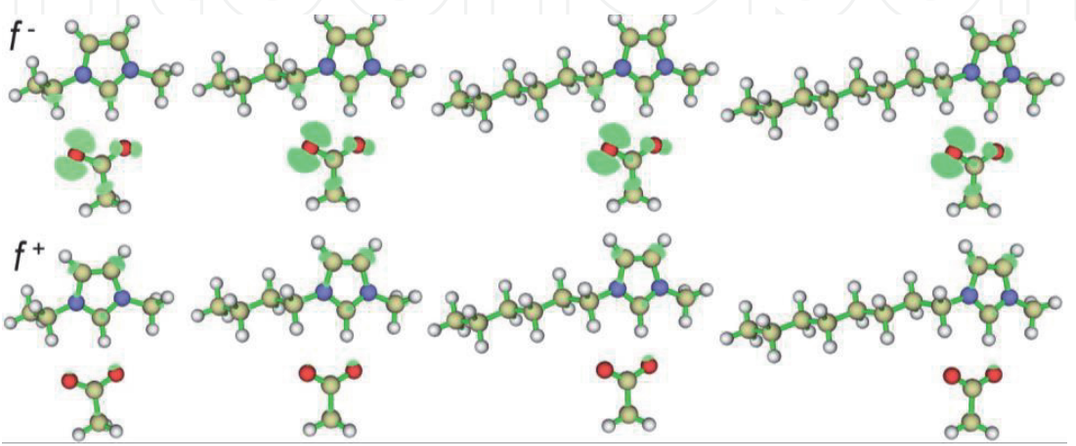

Figure 5.
Fukui index isosurfaces of [$C_n$mim]Ac (n = 2, 4, 6, 8) system with B3LYP/6-311++G(d,p) method. From left to right, it is [C_2mim]Ac, [C_4mim]Ac, [C_6mim]Ac and [C_8mim]Ac, respectively.

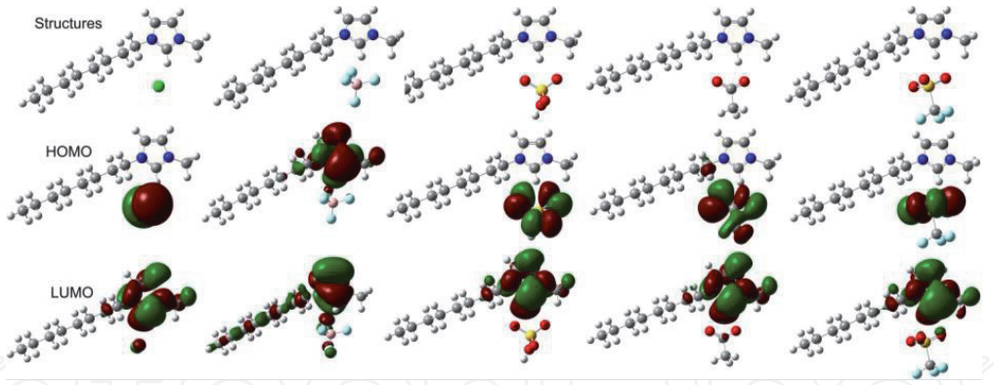

Figure 6.
Equilibrium geometry structures, HOMO and LUMO isosurfaces of [Omim]Y system with B3LYP/6-311++G (d, p) method. From left to right, it is [Omim]Cl, [Omim]BF_4, [Omim]HSO_4, [Omim]Ac and [Omim]TFO.

ILs	[Omim]Cl	[Omim]BF_4	[Omim]HSO_4	[Omim]Ac	[Omim]TfO
E_{HOMO}	−5.4007	−8.2613	−5.3992	−5.3951	−5.3943
E_{LUMO}	−0.9120	−1.4030	−0.9009	−0.8979	−0.8985
ΔE	4.4887	6.8583	4.4982	4.4972	4.4958

Table 5.
E_{HOMO}, E_{LUMO} *and* ΔE *(eV) of [Omim]Y with B3LYP/6-311++G(d, p) method.*

and form a feedback bond, which will make the imidazole ring stably adsorb on the iron surface. However, HOMO distribution of [Omim]Cl is very different. The HOMO of [Omim]BF_4 is mainly distributed on the imidazole ring and the alkyl group, and only a small amount of anions is distributed. The HOMO of [Omim]HSO_4, [Omim]Ac and [Omim]TFO are all allocated on anions, especially O atom. It is further stated that the oxygen-containing group easily forms a coordination bond with the d-orbit of the iron surface and is stably adsorbed on the iron surface.

The E_{HOMO}, E_{LUMO} and the energy gap ΔE of four [Omim]Y ionic liquids are shown in **Table 5**. It is shown in **Table 5** that the order of size of E_{HOMO} and E_{LUMO} is [Omim]TFO > [Omim]Ac > [Omim]HSO_4 > [Omim]Cl > [Omim]BF_4, which indicates that [Omim]TFO has the strongest ability to give electrons and [Emim]Cl has the strongest ability to get electrons. The order of ΔE is [Omim]BF_4 > [Omim]HSO_4 > [Omim]Ac > [Omim]TFO > [Omim]Cl, which indicates that [Omim]Cl has the best chemical activity and is the easiest to interact with metal surface.

3.3.2 Global active parameters

Table 6 shows the global activity parameters of [Omim]Y ionic liquids obtained by B3LYP/6-311++G(d, p) method. It is shown in **Table 6** that [Omim]HSO_4 has the largest dipole moment (μ), while [Omim]Ac has the smallest dipole moment (μ), indicating that [Omim]HSO_4 has the largest molecular polarity and easily interacts with the iron surface. For electronegativity (χ), the maximum of [Omim]BF_4 and the second of [Omim]TFO indicate that the ability of [Omim]BF_4 and [Omim]TFO to attract electrons is strong, which makes the molecules stably adsorbed on the iron surface by combining with the electrons on the iron surface. Global hardness (η) of [Omim]BF_4 is the largest, the global softness (S) is the smallest and the electrophilic index (ω) is the largest, indicating that [Omim]BF_4 is a good ionic liquid inhibitor. It can be seen from **Table 6** that the order of polarizability (α) is [Omim]TFO > [Omim]Ac > [Omim]HSO_4 > [Omim]BF_4 > [Omim]

ILs	μ/Debye	χ/eV	η/eV	S/eV^{-1}	ω	α(a.u.)
[Omim]Cl	12.2083	3.2213	2.0394	0.4903	2.5441	183.8247
[Omim]BF_4	12.2330	4.8321	3.4292	0.2916	3.4045	175.4047
[Omim]HSO_4	12.9717	3.8610	2.5009	0.3999	2.9804	195.8180
[Omim]Ac	9.5918	3.1464	2.2479	0.4449	2.2020	197.2063
[Omim]TfO	12.2888	4.1213	2.6048	0.3839	2.2604	204.3150

Table 6.
Global activity parameters for [Omim]Y system with B3LYP/6-311++G(d, p) method.

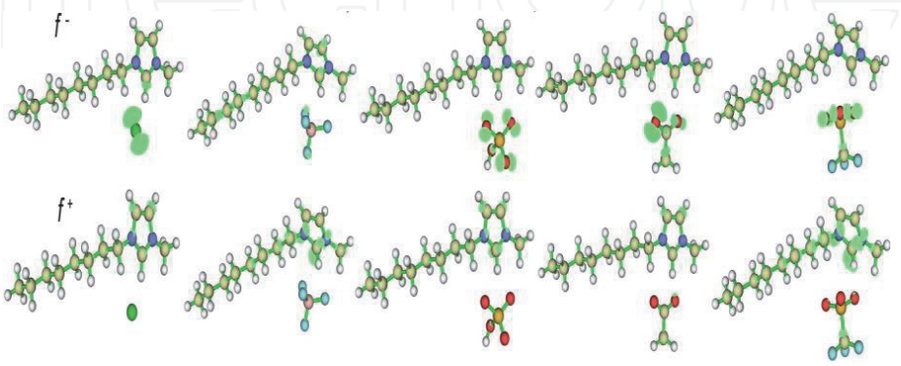

Figure 7.
Fukui index isosurfaces of [Omim]Y ionic liquids with B3LYP/6-311++G(d,p) method. From left to right, it is [Omim]Cl, [Omim]BF_4, [Omim]HSO_4, [Omim]Ac and [Omim]TFO.

Cl, indicating that [Omim]TFO is the most easily adsorbed on the iron surface, with the best corrosion inhibition effect and the highest corrosion inhibition efficiency.

3.3.3 Fukui index distribution

Figure 7 shows the Fukui index distribution of four ionic liquid [Omim]Y systems. From **Figure 7**, it can be seen that the electrophilic attack index of [Omim]Cl is mainly distributed on the Cl atom, and 2C (the number of atoms is shown in **Figure 1**) also has a small amount of the distribution. The nucleophilic attack index is allocated on 1N, 2C, 4C and 5C atoms. The electrophilic attack index of [Omim]BF_4 is 2C, 4C and F, and the electrophilic attack index is mainly distributed on 1N, 2C and 3N. Electric attack indexes of [Omim]HSO_4, [Omim]Ac and [Omim]TFO are mainly distributed on the O atom of anion, while the nucleophilic attack index is mainly distributed on the imidazole ring. In general, we found that the nucleophilic attack site of [Omim]Y is on the imidazole ring, and the electrophilic attack site is mainly on anion, especially O atom.

Compared with the HOMO and LUMO distribution of these three set ionic liquids systems of [$C_n$mim]Cl, [$C_n$mim]Ac and [Omim]Y in **Figures 2**, **4** and **6**, we found that the HOMO distribution is mainly located on the anion containing Cl and O atoms, while the LUMO distribution is mainly located on the imidazole ring of the cation. It shows that the anion containing Cl and O atom, and imidazole ring are the active regions of the ionic liquid. For E_{HOMO} and E_{LUMO}, the E_{HOMO} of [Omim]Cl is the largest, and the E_{LUMO} of [Omim]TFO is the smallest, indicating that [Omim]Cl has the strongest ability to give electrons and [Omim]TFO has the strongest ability to get electrons. The dipole moment (μ) of [Omim]HSO_4 is the largest, which indicates that the molecular polarity is the largest and it is easier to interact with the iron surface. For electronegativity (χ), the maximum is [Omim]BF_4 and the second is [Omim]TFO, which indicates that [Omim]BF_4 and [Omim]TFO have strong

ability to attract electrons. The global hardness (η) of [Omim]BF_4 and [Omim]TFO is larger, the global softness (S) is smaller and the electrophilic index (ω) is larger, which indicates that [Omim]BF_4 and [Omim]TFO are ionic liquids with better corrosion inhibition performance. For the polarizability (α), [Omim]TFO is the largest, which indicates that [Omim]TFO is the most easily adsorbed on the iron surface, and its corrosion inhibition effect is the best. In conclusion, [Omim]TFO has the best corrosion inhibition performance and the highest efficiency among the 11 ionic liquids studied.

4. Conclusion

The reaction activities such as E_{LUMO}, E_{HOMO}, the softness (S) and polarizability (α) increase gradually, whereas electronegativity (χ), energy gap (ΔE), hardness (η), dipole moment (μ) and electrophilic index (ω) of three sets ionic liquids 1-alkyl-3-methylimidazole chloride [$C_n$mim]Cl, 1-alkyl-3-methylimidazolium acetate [$C_n$mim]Ac and 1-octyl-3-methylimidazole salt [Omim]Y were studied by density functional theory. The results are as follows:

In [$C_n$mim]Cl and [$C_n$mim]Ac system, increasing the length of the alkyl chain, the HOMO energy E_{HOMO}, LUMO energy E_{LUMO}, softness (S) increase, while the dipole moment (μ), energy gap ΔE, electronegativity (χ), electrophilic index (ω), hardness (η) and polarizability (α) gradually decrease. In [Omim]Y (Y = Cl, BF_4, HSO_4, Ac, TFO) ionic liquids, the structure parameters of ionic liquids vary greatly with different anions.

The active region of [$C_n$mim]Cl system is the imidazole ring and anion Cl^-, while the [$C_n$mim]Ac system is located in the imidazole ring and the O atoms of anion. The active region of [Omim]Y system is located in the imidazole ring and an oxygen-containing group. The reaction is the active region of ionic liquid molecules will help interact with the iron surface and stably adsorb on the iron surface.

For [$C_n$mim]Cl system, the order of inhibition efficiency predicted is [C_8mim]Cl > [C_6mim]Cl > [C_4mim]Cl > [C_2mim]Cl, and [Omim]Cl may have the best inhibition effect. For [$C_n$mim]Ac system, the order of inhibition efficiency is [C_8mim]Ac > [C_6mim]Ac > [C_4mim]Ac > [C_2mim]Ac, and [Omim]Ac may have the best inhibition effect. Inhibition efficiency increases by increasing the alkyl chain length. For [Omim]Y system, [Omim]TFO may have better inhibition efficiency, and the sequence of inhibition efficiency needs further study.

Acknowledgements

This work was supported in part by the National Natural Science Foundation of China (51774158, 5126402) and Back-up Personnel Foundation of Academic and Technology Leaders of Yunnan Province (2011HR013).

Conflict of interest

The authors declare no conflict of interest.

DOI: http://dx.doi.org/10.5772/intechopen.92768

Author details

Guocai Tian* and Weizhong Zhou
State Key Laboratory of Complex Nonferrous Metal Resource Clean Utilization, Faculty of Metallurgical and Energy Engineering, Kunming University of Science and Technology, Yunnan, Kunming, China

*Address all correspondence to: tiangc@kust.edu.cn

References

[1] Zhang TS, Zhang H, Gao H. Inhibitors. Beijing: Chemical Industry Press; 2008. pp. 316-339

[2] Li WH. Synthesis and Evaluation of New Corrosion Inhibitors. Beijing: Science Press; 2015. pp. 1-40

[3] Wen X, Bai P, Luo B, Zheng S, Chen C. Review of recent progress in the study of corrosion products of steels in a hydrogen sulphide environment. Corrosion Science. 2018;**139**:124-140. DOI: 10.1016/j.corsci.2018.05.002

[4] Antonijevic MM, Petrovic MB. Copper corrosion inhibitors. A review. International Journal of Electrochemistry. 2008;**3**:1-28

[5] Li RX. Synthesis and Application of Green Solvent-Ionic Liquids. Beijing: Chemical Engineering Press; 2004. pp. 2-10

[6] Deng Y. Ionic Liquid-Property, Preparation and Application. Beijing: China Petrochemical Press; 2006. pp. 10-23

[7] Zhang SJ, Lv XM, Liu ZP. Ionic Liquids: From Basic Research to Industrial Applications. Beijing: Science Publishing; 2006. pp. 50-380

[8] Verma C, Ebenso EE, Quraishi MA. Ionic liquids as green and sustainable corrosion inhibitors for metals and alloys: An overview. Journal of Molecular Liquids. 2017;**233**:403-414. DOI: 10.1016/j.molliq.2017.02.111

[9] Kesavan D, Gopiraman M, Sulochana N. Green inhibitors for corrosion of metals: A review. Chemical Science Review and Letters. 2012;**1**(1): 1-8

[10] Quan KY. Research on the Method and Application of Strong Polarization Detection of Metal Corrosion. Chongqing: Chongqing University; 2018. pp. 8-12

[11] Verma C, Ebenso EE, Bahadur I, Quraishi MA. An overview on plant extracts as environmental sustainable and green corrosion inhibitors for metals and alloys in aggressive corrosive media. Journal of Molecular Liquids. 2018;**266**:577-590. DOI: 10.1016/j.molliq.2018.06.110

[12] Zarrouk A, Messali M, Zarrok H. Synthesis, characterization and comparative study of new functionalized imidazolium-based ionic liquids derivatives towards corrosion of C38 steel in molar hydrochloric acid. International Journal of Electrochemical Science. 2012;**7**:6998-7015

[13] Zheng X, Zhang S, Li W, Yin L, He J, Wu J. Investigation of 1-butyl-3-methyl-1-H-benzimidazolium iodide as inhibitor for mild steel in sulfuric acid solution. Corrosion Science. 2014;**80**:383-392. DOI: 10.1016/j.corsci.2013.11.053

[14] Kowsari E, Payami M, Amini R, et al. Task-specific ionic liquid as a new green inhibitor of mild steel corrosion. Applied Surface Science. 2014:478-486. DOI: 10.1016/j.apsusc.2013.11.017

[15] Lozano I, Mazario E, Olivaresxometl CO, et al. Corrosion behaviour of API 5LX52 steel in HCl and H_2SO_4 media in the presence of 1,3-dibencilimidazolio acetate and 1,3-dibencilimidazolio dodecanoate ionic liquids as inhibitors. Materials Chemistry and Physics. 2014;**147**(1): 191-197. DOI: 10.1016/j.matchemphys.2014.04.029

[16] Zheng X, Zhang S, Gong M, et al. Experimental and theoretical study on the corrosion inhibition of mild steel by 1-octyl-3-methylimidazolium l-prolinate in sulfuric acid solution. Industrial & Engineering Chemistry

Research. 2014;**53**(42):16349-16358. DOI: 10.1021/ie502578q

[17] Zhang QB, Hua YX. Corrosion inhibition of mild steel by alkylimidazolium ionic liquids in hydrochloric acid. Electrochimica Acta. 2009;**54**(6):1881-1887. DOI: 10.1016/j.electacta.2008.10.025

[18] Ma Y, Han F, Li Z, et al. Corrosion behavior of metallic materials in acidic-functionalized ionic liquids. ACS Sustainable Chemistry & Engineering. 2016;**4**(2):633-639. DOI: 10.1021/acssuschemeng.5b00974

[19] Olivaresxometl O, Lopezaguilar C, Herrastigonzalez P, et al. Adsorption and corrosion inhibition performance by three new ionic liquids on API 5lA52 steel surface in acid media. Industrial & Engineering Chemistry Research. 2014; **53**(23):9534-9543. DOI: 10.1021/ie4035847

[20] Ma Y, Han F, Li Z, et al. Acidic-functionalized ionic liquid as corrosion inhibitor for 304 stainless steel in aqueous sulfuric acid. ACS Sustainable Chemistry & Engineering. 2016;**4**(9): 5046-5052. DOI: 10.1021/acssuschemeng.6b01492

[21] Feng L. Experimental and theoretical studies of 1-vinyl-3-hexylimidazolium iodide ([VHIM]I) as corrosion inhibitor for the mild steel in sulfuric acid solution. International Journal of Electrochemical Science. 2017:1915-1928. DOI: 10.20964/2017.03.30

[22] Verma C, Obot IB, Bahadur I, et al. Choline based ionic liquids as sustainable corrosion inhibitors on mild steel surface in acidic medium: Gravimetric, electrochemical, surface morphology, DFT and Monte Carlo simulation studies. Applied Surface Science. 2018:134-149. DOI: 10.1016/j.apsusc.2018.06.035

[23] Verma C, Olasunkanmi LO, Bahadur I, et al. Experimental, density functional theory and molecular dynamics supported adsorption behavior of environmental benign imidazolium based ionic liquids on mild steel surface in acidic medium. Journal of Molecular Liquids. 2019;**273**:1-15. DOI: 10.1016/j.molliq.2018.09.139

[24] Arellanes-Lozada P, Olivares-Xometl O, Likhanova NV. Adsorption and performance of ammonium-based ionic liquids as corrosion inhibitors of steel. Journal of Molecular Liquids. 2018;**265**:151-163. DOI: 10.1016/j.molliq.2018.04.153

[25] Likhanova NV, Arellanes-Lozada P, Olivares-Xometl O. Effect of organic anions on ionic liquids as corrosion inhibitors of steel in sulfuric acid solution. Journal of Molecular Liquids. 2019;**279**:267-278. DOI: 10.1016/j.molliq.2019.01.126

[26] Gece G. The use of quantum chemical methods in corrosion inhibitor studies. Corrosion Science. 2008;**50**(11): 2981-2992. DOI: 10.1016/j.corsci.2008.08.043

[27] Murulana LC, Singh AK, Shukla SK, Kabanda MM, Ebenso EE. Experimental and quantum chemical studies of some bis(trifluoromethyl-sulfonyl) imide imidazolium- based ionic liquids as corrosion inhibitors for mild steel in hydrochloric acid solution. Industrial & Engineering Chemistry Research. 2012; **51**(40):13282-13299. DOI: 10.1021/ie300977d

[28] Sasikumar Y, Adekunle AS, Olasunkanmi LO, Bahadur I, Baskar R, Kabanda MM, et al. Experimental, quantum chemical and Monte Carlo simulation studies on the corrosion inhibition of some alkyl imidazolium ionic liquids containing tetrafluoroborate anion on mild steel in acidic medium. Journal of Molecular Liquids. 2015;**211**:105-118. DOI: 10.1016/j.molliq.2015.06.052

[29] Mashuga ME, Olasunkanmi L, Adekunle AS, Yesudass S, Kabanda MM, Ebenso EE. Adsorption, thermodynamic and quantum chemical studies of 1-hexyl-3-methyl-imidazolium based ionic liquids as corrosion inhibitors for mild steel in HCl. Materials. 2015;**8**(6): 3607-3632. DOI: 10.3390/ma8063607

[30] Yesudass S, Olasunkanmi LO, Bahadur I, Kabande MM, Obot IB, Ebenso EE. Experimental and theoretical studies on some selected ionic liquids with different cations/anions as corrosion inhibitors for mild steel in acidic medium. Journal of the Taiwan Institute of Chemical Engineers. 2016;**64**:252-268. DOI: 10.1016/j.jtice.2016.04.006

[31] Frisch MJ, Trucks GW, Schlegel HB, Scuseria GE, Robb MA, Cheeseman JR, et al. Gaussian 09, Revision B.02. Wallingford CT: Gaussian, Inc.; 2009

[32] Lu T, Chen F. Multiwfn: A multifunctional wavefunction analyzer. Journal of Computational Chemistry. 2012;**33**(5):580-592. DOI: 10.1002/jcc.22885

[33] Lu T, Chen F. Quantitative analysis of molecular surface based on improved marching tetrahedra algorithm. Journal of Molecular Graphics and Modelling. 2012;**38**:314-323. DOI: 10.1016/j.jmgm.2012.07.004

[34] Zhao HX, Zhang XH, Ji L, Hu HX, Li QS. Quantitative structure–activity relationship model for amino acids as corrosion inhibitors based on the support vector machine and molecular design. Corrosion Science. 2014;**83**: 261-271. DOI: 10.1016/j.corsci.2014.02.023

[35] Daoud D, Douadi T, Hamani H, Chafaa S, Al-Noaimi M. Corrosion inhibition of mild steel by two new S-heterocyclic compounds in 1 M HCl: Experimental and computational study. Corrosion Science. 2015;**94**:21-37. DOI: 10.1016/j.corsci.2015.01.025

[36] Koopmans T. Ordering of wave functions and eigenenergies to the individual electrons of an atom. Physica. 1933;**1**(1):104-113

[37] Yang W, Parr RG. Hardness, softness, and the Fukui function in the electronic theory of metals and catalysis. Proceedings of the National Academy of Sciences of the United States of America. 1985;**82**(20):6723-6726. DOI: 10.1073/pnas.82.20.6723

[38] Chermette H. Chemical reactivity indexes in density functional theory. Journal of Computational Chemistry. 1999;**20**(1):129-154. DOI: 10.1002/(sici)1096-987x(19990115)20:1<129::aid-jcc13>3.0.co;2-a

[39] Obot IB, Macdonald DD, Gasem ZM. Density functional theory (DFT) as a powerful tool for designing new organic corrosion inhibitors. Part 1: An overview. Corrosion Science. 2015; **99**:1-30. DOI: 10.1016/j.corsci.2015.01.037

[40] Li XH, Deng SD, Fu H, Li TH. Adsorption and inhibition effect of 6-benzyl-aminopurine on cold rolled steel in 1.0 M HCl. Electrochimica Acta. 2009;**54**(16):4089-4098. DOI: 10.1016/j.electacta.2009.02.084

[41] Parr RG, Chattaraj PK. Principle of maximum hardness. Journal of the American Chemical Society. 1991; **113**(5):1854-1855. DOI: 10.1021/ja00005a072

[42] Parr R, Yang W. Density Functional Theory of Atoms and Molecules. New York: Oxford Science Publications; 1989

[43] Guo L, Ren XL, Zhou Y, Xu SY, Gong YL, Zhang ST. Theoretical evaluation of the corrosion inhibition performance of 1,3-thiazole and its amino derivatives. Arabian Journal of Chemistry. 2017;**10**(1):121-130. DOI: 10.1016/j.arabjc.2015.01.005

[44] Shahraki M, Dehdab M, Elmi S. Theoretical studies on the corrosion inhibition performance of three amine derivatives on carbon steel: Molecular dynamics simulation and density functional theory approaches. Journal of the Taiwan Institute of Chemical Engineers. 2016;**62**:313-321. DOI: 10.1016/j.jtice.2016.02.010

[45] Fukui K. Role of frontier orbitals in chemical reactions. Science. 1982; **218**(4574):747-754. DOI: 10.1126/science.218.4574.747

[46] Saha SK, Hens A, Murmu NC, Banerjee P. A comparative density functional theory and molecular dynamics simulation studies of the corrosion inhibitory action of two novel N-heterocyclic organic compounds along with a few others over steel surface. Journal of Molecular Liquids. 2016;**215**:486-495. DOI: 10.1016/j.molliq.2016.01.024